ANALYSIS OF DIFFERENT EARTHQUAKE RECORDS ON THE BEHAVIOUR OF CIRCULAR TUNNEL IN SANDY SOIL

Farouk, M.A.[1*], **Abo-Alanwar, M.M.**[2], **Elbatal, S.A.**[2]

1 Civil Engineering Department, El Gazeera Higher Institute for Engineering and Technology, Cairo, Egypt.

2 Civil Engineering Department, Faculty of Engineering, Al-Azhar University, Cairo, Egypt.

*Correspondence: mahmoud.farouk2018@gmail.com

ABSTRACT

Underground facilities serve several purposes as an essential part of the infrastructure of modern society. Subways, railroads, highways, material storage, sewage, and water transportation are applications of tunnels. Recently, increase in the frequency and magnitude of earthquakes have led to focus on the actual behavior of underground tunnels not only under static loads but also under dynamic effect of earthquakes. This study investigated 2D-numerical model circular tunnels under the influence of different earthquake records for sandy soils with different consistes. The soil types were dense, medium dense and loose sandy soils were studied. Three earthquake records, varying in peak ground acceleration (PGA) values and duration [Olympia earthquake (PGA= 0.16g and T= 89.08sec), Kalamata earthquake (PGA= 0.331g and T= 25.88sec) and Northridge earthquake (PGA=0.883g and T= 59.98sec)] have been conducted. A parametric study for circular tunnels in different soil states under static load and earthquake dynamic loads was examined. Specific points were observed to monitor deformations and stresses. Comparing the behaviour of tunnels under static load and earthquake has been illustrated. The analysis of results shows that the duration of earthquake records has a greater impact on horizontal displacement than PGA values. Peak ground acceleration (PGA) significantly affects vertical displacements, bending moments and axial forces. Axial forces are almost constant under earthquake records with PGA less than 0.331g, whereas PGA more than 0.331g increases slightly. Finally, the effect of earthquake records should be considered in tunnels behaviour and design to avoid permanent deformation, stresses or collapse of the tunnels.

KEYWORDS: Earthquake records, Tunnel, Sandy soil, Behavior, Plaxis 2D, Peak ground acceleration.

التحليل لسجلات زلازل مختلفة على سلوك نفق دائرى في التربة الرملية

محمود فاروق عارف[1]* ، محمد أبو الانوار محمود[2] ، سامح البطل عبد الحليم[2]

[1] قسم الهندسة المدنية، معهد الجزيرة العالي للهندسة والتكنولوجيا، القاهرة، مصر.

[2] قسم الهندسة المدنية، كلية الهندسة، جامعة الأزهر، القاهرة، مصر.

*البريد الاليكتروني للباحث الرئيسي : mahmoud.farouk2018@gmail.com

الملخص

البنية التحتية تخدم أغراضًا عديدة وتعتبر جزءًا أساسيًا من البنية التحتية للمجتمعات الحديثة. الأنفاق والسكك الحديدية والطرق السريعة وتخزين المواد والصرف الصحي ونقل المياه هي إستخدامات للأنفاق. مؤخرًا، أدى زيادة تكرار وشدة الزلازل إلى التركيز على سلوك الأنفاق ليس فقط تحت الأحمال الثابتة ولكن أيضًا بالإضافة إلى التأثير الديناميكي للزلازل. في هذا البحث تم دراسة نموذج ثنائي الأبعاد لنفق دائري تحت تأثير سجلات زلزالية مختلفة علي تربة رملية ذات قوام مختلف. تمت الدراسة علي رمل كثيف ومتوسط الكثافة وسائب. تمت تطبيق ثلاث سجلات زلزالية مختلفة، تختلف في قيم ذروة التسارع (PGA) والمدة [زلزال أوليمبيا (PGA =0.16g) ، الزمن=89.08 ثانية)، وزلزال كالاماتا (PGA =0.331g، الزمن=25.88 ثانية) وزلزال نورثريدج (PGA= 0.883g ، الزمن =59.98 ثانية)]. تمت دراسة سلوك نفق دائري تحت الأحمال الساكنة والتأثير الديناميكي لمعاملات زلازل مسجلة. تم ملاحظة نقاط محددة لمراقبة التشكلات والتشوهات والإجهادات. تم عمل مقارنة لسلوك الأنفاق تحت الأحمال الساكنة وسجلات الزلازل. تحليل النتائج أظهرت أن مدة الزلازل لها تأثير أكبر على التشكل والتشوه الأفقي بينما قيم PGA التسارع الأفقي الأقصى تؤثر بشكل كبير على التشكلات والتشوهات الرأسية وعزم الانحناء وقوى الشد المحورية. مع ملاحظة أن قوى الشد المحورية تقريبا تكون ثابتة

Analysis of Different Earthquake Records on The Behaviour of Circular Tunnel in Sandy Soil

تحت الزلازل بقيم PGA أقل من0.331g، في حين تزيد قليلاً مع PGA أكبر من 0.331g . أخيرًا، يجب أخذ تأثير سجلات الزلازل في سلوك الأنفاق وتصميمها فى الاعتبار لتجنب التشكل والتشوهات الدائمة والإجهادات وإنهيار الأنفاق.

الكلمات المفتاحية : سجلات الزلازل، النفق، التربة الرملية، السلوك، Plaxis 2D، ذروة التسارع الأرضى .

1. INTRODUCTION

In the last few decades, the construction of tunnels has significantly increased. Some of these tunnels are constructed in seismic regions. Tunnel construction is in densely populated urban areas and metropolises to meet the growing demand for space and passage. Various types of dynamic loading conditions, such as impact load, blast load, and seismic stress, may be imposed on tunnels. Due to the demand for infrastructure, it can sometimes be challenging to avoid building tunnels in areas that have previously experienced earthquakes. If these infrastructures are not properly planned with the effects of earthquakes in mind, they may suffer damage. Analysis, design, construction, operation and damage assessment must carefully consider the impact of seismic loading. Each seismic activity in that region increases the likelihood that these infrastructures may be damaged.

Dynamic FEM analysis results for tunnel portals indicated that the largest force acting on the lining occurs near the tunnel portal when an earthquake wave propagates parallel to the tunnel axis [1]. Finite difference analysis showed that, the results of the analytical closed form and the numerical solution are in excellent agreement. The study findings and some feasible recommendations for utilizing closed-form solutions were presented [2]. Despite underground structures being more resilient to seismic excitation compared to surface structures, were still at risk of damage during a major earthquake, particularly if they were built in a fluid layer [3]. A study on seismic analysis of a crucial water tunnel facility in the San Francisco Bay Area using modeling and simulations demonstrated that, the tunnel met seismic performance goals across various analysis methods [4]. Dynamic behavior of circular tunnels in the transverse direction using various methods. The cases examined concern a short tunnel that was dug in two distinct clayey deposits. According to the plasticity assessments, a seismic event caused a significant change in the loads operating on the lining, resulting in continuous increases in the hoop force and bending moment [5]. A study used the ABAQUS v.6.8 program to present an idealized two-dimensional plane strain finite element seismic soil-tunnel interaction analysis. Three ground motion records were used to show seismic motions with low, intermediate, and high-frequency content. Two types of sandy soil were modeled. The results showed that the tunnel amplifies seismic waves on the soil surface, with the greatest amplification occurring at the tunnel–soil interface [6].

Analysis for the seismic interaction between the surrounding soil and tunnels demonstrate that, the maximum straining actions in the tunnel lining are anti-correlated with the relative stiffness between the tunnel and the surrounding soil. The tunnel's location and peak ground acceleration have a significant impact. In regions with peak ground acceleration larger than 0.15g, seismic analysis should be considered [7]. Examination for seismic analysis impact on tunnel systems in Greater Cairo metro line No.4, Phase No.1. indicate that, seismic waves lead to heightened displacement and notable alterations in internal forces, particularly in shear force and bending moment, with minimal impact on the normal force of tunnel lining [8]. A finite element analysis used to investigate the response of a shallow tunnel in soft ground under seismic conditions.

It was observed that the deformation of the tunnel lining is influenced by the depth of embedment and the flexibility ratio of the tunnel. Ovaling (in a circular tunnel) and racking (in a rectangular tunnel) decrease significantly when the embedment ratio exceeds 2 [9]. The accuracy of underground infrastructure risk assessment and seismic fragility curves for circular tunnels under moderate to powerful earthquake was investigated, and the derived fragility curves were found to fit well with the empirical curves based on seismic damage seen in tunnels [10].
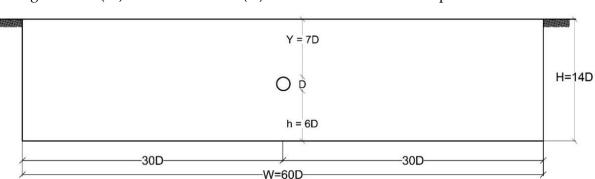
Finite element modeling of the in situ situation, which was validated by experimental results to demonstrate tunnel deformation behavior under static loading conditions in soft rocks. Using Abaqus, 3D nonlinear finite element analysis was performed. The results indicated that tunnel diameter, overburden depth, and rock weathering indicate the stability of tunnels under severe loading conditions [11]. A study carried out on concrete pipe behavior during seismic shaking showed that, linear elastic and Mohr-Coulomb models had lower bending moments than hardening soil and hardening soil with small strain stiffness models [12]. Results of ANSYS for numerical simulations showed that, arch crown deformation at 3.8 cm and wall corner stress at 2.6×10^7 Pa [13]. A study on Delhi metro tunnel behavior under various dynamic loading cases showes that, combined earthquake and train motion cause larger displacements in soil and forces in tunnel liners compared to individual loads [14].

Underground structures, like tunnels, need more accurate analysis and design in case of earthquakes to prevent damage and excess deformation. This study investigates the behavior of tunnel in sandy soil with different earthquake records.

2. Details of finite element analyses

In the present study, a finite element package of PLAXIS 2D version 21 [15] is used to simulate a Non-linear numerical model of a circular tunnel embedded in sandy soil with different consistencies. The study aims to investigate and analyze the influence of static loads and different earthquake records on a circular tunnel in different type of sandy soil. Soil elements were selected as plane strains with 15-node triangular elements. The sandy soil is presented as a hardening soil model with a small strain stiffness (HS small). **Table 1** shows the properties of the used different soil states. Concrete tunnel lining was selected of Plate with 5-node beam elements. **Table 2** shows the properties of the used concrete material tunnel lining. The model dimensions were taken as 60D wide and 14D high, where D = diameter of the tunnel. For all investigated cases, the diameter of the tunnel was D = 9.00 m with lining thickness (t) = 0.45 m and the tunnel embedded under the ground surface with Cover (Y) = 7D, where Y is the tunnel location measured from the ground surface and crown of the tunnel as shown in **Fig. 1**.

One of the most important steps in the analysis is the definition of all loads, lining material and soil types that affect behaviour of the model. Different types of loads were used in this study. These types can be classified as static loads (own weight of the model elements) and three earthquake records, varying in peak ground acceleration (PGA) values and duration [Olympia earthquake (PGA = 0.16 g and duration = 89.08 sec), Kalamata earthquake (PGA = 0.331 g and duration = 25.88 sec) and Northridge earthquake (PGA = 0.883 g and duration = 59.98 sec)] as shown in **Table 3** and **Fig. 2** show the earthquake time with a dynamic multiplier (accelerations). The parametric study conducted in this analysis is presented in **Table 4**.

The horizontal displacement (δ_x), vertical displacement (δ_y), radial displacement (δ_r), bending moment (M) and normal force (N) were determined and compared.

Fig. 1. Dimensions of the numerical model.

Table 1. Properties of different types of used soil.

Property	Dense sand (S1)	Medium dense sand (S2)	Loose sand (S3)	Units
Relative density (R_D)	80	50	25	(%)
γ_{unsat}	18.2	17.0	16.0	(kN/m³)
γ_{sat}	20.3	19.8	19.4	(kN/m³)
E_{50}^{ref}	48×10^3	30×10^3	15×10^3	(kN/m²)
E_{oed}^{ref}	48×10^3	30×10^3	15×10^3	(kN/m²)
E_{ur}^{ref}	144×10^3	90×10^3	45×10^3	(kN/m²)
G_0^{ref}	114×10^3	94×10^3	77×10^3	-------
m	0.45	0.544	0.622	-------
$\gamma_{0.7}$	1.2×10^{-4}	1.5×10^{-4}	1.8×10^{-4}	(kN/m³)
φ	38	34.3	31.1	(°)
ψ	8	4.3	1.1	(°)
R_f	0.90	0.938	0.969	-------

Table 2. Material characteristics of the tunnel lining.

Parameter	Symbol	Value	Units
Material type	Elastic	-------	-------
Young's modulus	E	22×10^6	(kN / m²)
Concrete density	γ	25.0	(kN / m³)
Thickness	t	0.45	m
Poisson ratio	ν	0.20	-------
Normal stiffness	EA	9.9×10^6	kN/m
Flexural rigidity	EI	167.1×10^3	kN.m²/m
Weight	w	11.25	kN/m/m

Table 3. Properties of selected Earthquake records [16].

No.	Earthquake record	Duration (sec)	PGA	PGA at time
1	Olympia earthquake (EQ1)	89.08	0.16 g	10.96 sec
2	Kalamata earthquake (EQ2)	25.88	0.331 g	3.27 sec
3	Northridge earthquake (EQ3)	59.98	0.883 g	9.82 sec

(g =acceleration due to Earth's gravity) (1 g = 9.81 m/s^2)

Fig. 2. Acceleration time history for (A) Olympia earthquake record, (B) Kalamata earthquake record and (C) Northridge earthquake record.

Table 4. Details of finite element models.

Diameter	Thickness	Cover	Soil type	Loads
9.00 m	0.05 D	7.00 D	Dense sand (S1)	Static.
			Medium-dense sand (S2)	Olympia record (EQ1). Kalamata record (EQ2).
			Loose sand (S3)	Northridge record (EQ3).

3. Numerical results

From the parametric study, horizontal displacement, vertical displacement, radial displacement, bending moment and normal force are obtained and represented in the following mathematical form:

- Horizontal displacement as a ratio of tunnel diameter : δ_x / D %

- Vertical displacement as a ratio of tunnel diameter : δ_y / D %

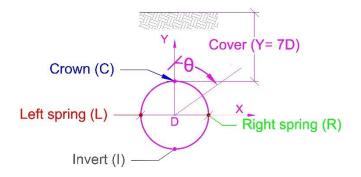- Radial displacement as a ratio of tunnel diameter : δ_r / D %

- Bending moment coefficient:

$$\alpha = \frac{4\,M}{\gamma\,C\,D^2} \quad \text{Eq.1} \quad [17]$$

- Normal force coefficient:

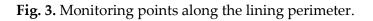$$\beta = \frac{2\,N}{\gamma\,C\,D} \quad \text{Eq.2} \quad [18]$$

Where: M = Bending moment in the lining (kN.m/m), N = Normal force in the lining (kN/m), γ = Unsaturated unit weight of soil (kN/m³), C = The tunnel location measured from the ground surface and crown of the tunnel (m) and D = Diameter of tunnel (m).

The obtained results were divided into the following categories:

3.1. Response of Monitoring Points during the Earthquake

Four points; crown point, invert point, right spring point and left spring point, were selected to study the behaviour of tunnel lining for all cases.
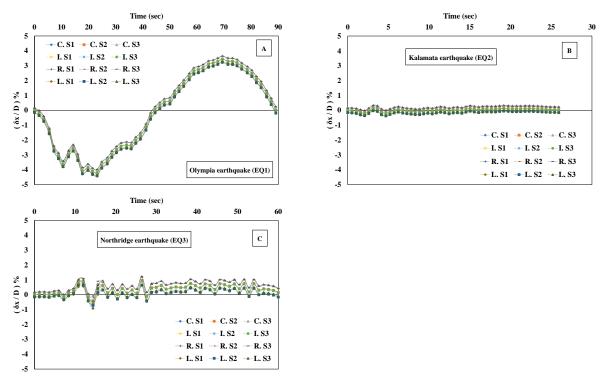

Fig. 3. Monitoring points along the lining perimeter.

Fig. 4. Dynamic horizontal displacements as a ratio of tunnel diameter of monitoring points for different soil states during (A) Olympia earthquake, (B) Kalamata earthquake and (C) Northridge earthquake.

Fig. 4A shows the dynamic horizontal displacement as a ratio of tunnel diameter for monitoring points subjected to the Olympia earthquake record in various soil types. For all points and cases, the static deformation is nearly 0.0, reaching 4.36% at 23.12 seconds, then returning to zero at 45 seconds. It increases to 3.63% at 69.36 seconds before returning to static deformation at the end of the earthquake.

Fig. 4B shows the dynamic horizontal displacement as a ratio of tunnel diameter for monitoring points subjected to the Kalamata earthquake record in various soil types. For all points and cases, the static deformation is nearly 0.0, reaching 0.35% at 4.67 seconds, then returning almost zero at 15 seconds, then returning to static deformation at the end of the earthquake.

Fig. 4C shows the dynamic horizontal displacement as a ratio of tunnel diameter for monitoring points subjected to the Northridge earthquake record in various soil types. For all points and cases, the static deformation is nearly 0.0, reaching 1.09% at 12 seconds and decreasing to 0.89% at 14.39 seconds, returning 1.17 % at 26.39 seconds, and becoming around 1% at 30 seconds until the end of the earthquake.
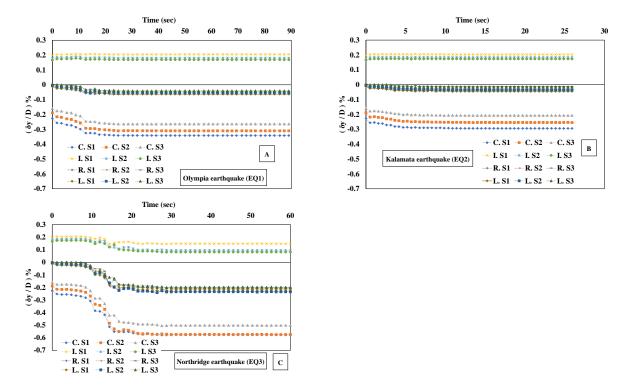
Fig. 5. Dynamic vertical displacements as a ratio of tunnel diameter of monitoring points for different soil states during (A) Olympia earthquake, (B) Kalamata earthquake and (C) Northridge earthquake.

Fig. 5A and Fig. 5B show the dynamic vertical displacements as a ratio of tunnel diameter for monitoring points in different soil states subjected to the Olympia earthquake record and the Kalamata earthquake record. It started with negative values from static deformation for crown point, right spring point, and left spring point cases and increased until around peak ground acceleration, then became constant till the end of the earthquake record. In addition, invert points started with positive values from static deformation and continued constant till the end of the earthquake record.

Fig. 5C shows the dynamic vertical displacement as a ratio of tunnel diameter for monitoring points in different soil states subjected to the Northridge earthquake record. It started with negative values from static deformation for crown point, right spring point, and left spring point cases, slightly increased to peak ground acceleration, continued with more increasing till 18 seconds, and became constant till the end of the earthquake record. In addition, invert points started with positive values from static deformation and slightly increased until 18 seconds then continued constant till the end of the earthquake record.
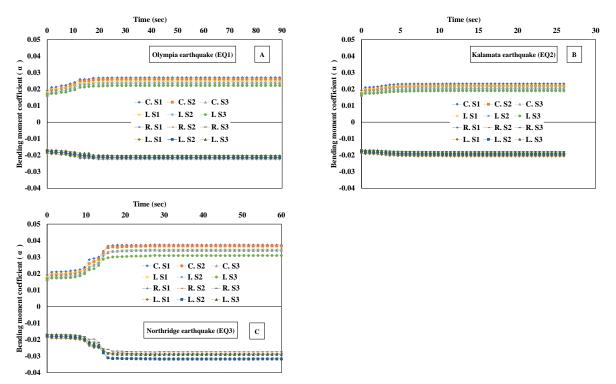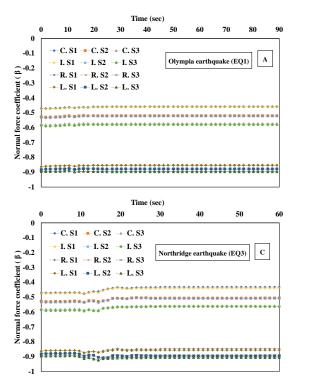
Fig. 6. Dynamic bending moment coefficient (α) of monitoring points for different soil states during (A) Olympia earthquake, (B) Kalamata earthquake and (C) Northridge earthquake.

Fig. 6A and Fig. 6B show the dynamic bending moment coefficient (α) for monitoring points in different soil states subjected to the Olympia earthquake record and the Kalamata earthquake record. It started with positive values from static deformation for crown point and invert point cases and increased until around peak ground acceleration, then became constant until the end of the earthquake record. In addition, the right spring point and left spring point cases started with negative values from static deformation, slightly increased to peak ground acceleration, and became constant till the end of the earthquake record.

Fig. 6C shows the dynamic bending moment coefficient (α) for monitoring points in different soil states subjected to the Northridge earthquake record. It started with positive values from static deformation for crown point and invert point cases and increased until around peak ground acceleration, then became constant until the end of the earthquake record. In addition, right spring point and left spring point cases started with negative values from static deformation and increased until around peak ground acceleration then became constant till the end of the earthquake record.
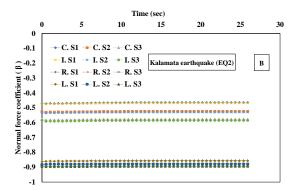
Fig. 7. Dynamic normal force coefficient (β) of monitoring points for different soil states during
(A) Olympia earthquake, (B) Kalamata earthquake and
(C) Northridge earthquake.

Fig. 7A and Fig. 7B show the dynamic normal force coefficient (β) for monitoring points in different soil states subjected to the Olympia earthquake record and Kalamata earthquake record. For all points and cases, it started with negative values from static deformation and then became constant until the end of the earthquake record.

Fig. 7C shows the dynamic normal force coefficient (β) for monitoring points in different soil states subjected to the Northridge earthquake record. For all points and cases, it started with negative values from static deformation, slightly increased to peak ground acceleration and became constant till the end of the earthquake record.

3.2. Deformations and stresses of tunnel lining at the end of the earthquake records

The deformations and stresses at the end of the earthquake were measured for all points along the perimeter starting from the crown point (θ =0°) in a clockwise direction.
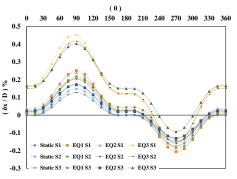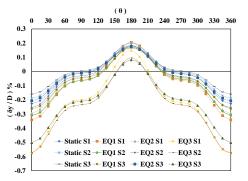

Fig. 8. Comparison between horizontal displacements along tunnel lining for different soil states subjected to static load and different earthquake records.

Fig. 8 shows the horizontal displacement along the tunnel lining. In case of static load for all different soil states, it has positive values except around θ=195° to 345° which were negative. Whereas, in case of EQ1 and EQ2, for all different soil states, they have positive values except around θ=210° to 330° which were negative. In addition, in the case of EQ3, all values were positive except around θ=240° to 300° which were negative for all different soil states.
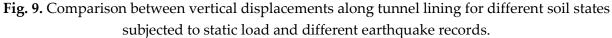

Fig. 9. Comparison between vertical displacements along tunnel lining for different soil states subjected to static load and different earthquake records.

Fig. 9 shows the vertical displacement along the tunnel lining. In cases of static load, EQ1, and EQ2, the values were negative except around θ=120° to 240°, where they were positive for all different soil states. Whereas, in case of EQ3, for all different soil states, they have negative values except around θ = 150° to 210° which were positive.
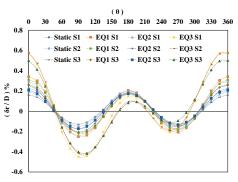

Fig. 10. Comparison between radial displacements along tunnel lining for different soil states subjected to static load and different earthquake records.

Fig. 10 shows the radial displacement along the tunnel lining. In case of static load, EQ1 and EQ2 for all different soil states have positive values except around θ=45° to 135° and θ=225° to 310°, values were negative. Whereas, in case of EQ3, for all different soil states, they have positive values except around θ=45° to 165° and θ=210° to 290° where the values were negative.
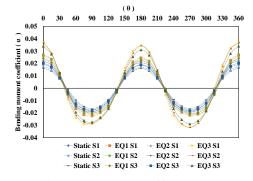

Fig. 11. Comparison between bending moment coefficient (α) along tunnel lining for different soil states subjected to static load and different earthquake records.

Fig. 11 shows the bending moment coefficient (α) along the tunnel lining. In case of static load and earthquake records for all types of soil, it has positive values except around θ=40° to 135° and θ=225° to 315°, it has negative values.
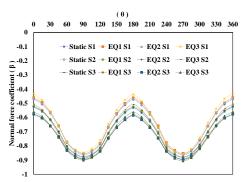

Fig. 12. Comparison between normal force coefficient (β) along tunnel lining for different soil states subjected to static load and different earthquake records.

Fig. 12 shows the normal force coefficient (β) along the tunnel lining. In case of static load and earthquake records for all types of soil, it has negative values.

4. Analysis of results

Analysis of the obtained results has been conducted to evaluate the tunnel lining behaviour as follows:
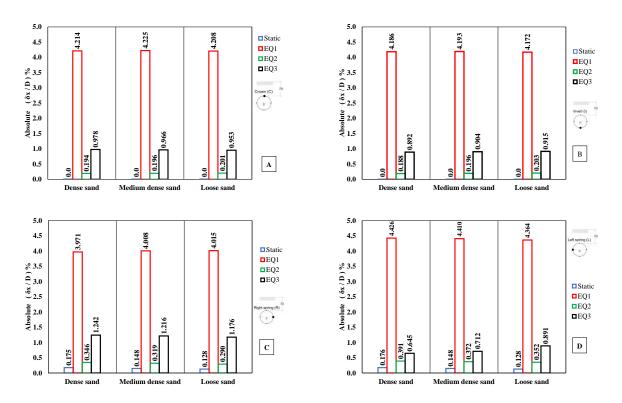

Fig. 13. Absolute maximum horizontal displacements for different soil states subjected to static load and different earthquake records for (A) Crown point, (B) Invert point, (C) Right spring point and (D) Left spring point.

Fig. 13 show the absolute maximum horizontal displacements for monitoring points as the percentage ratio of tunnel diameter (δ_x/D%) for different soil states under static load and earthquake records. For the static load case, where no seismic activity is considered, the horizontal displacement is found to be zero at the crown point and invert point of the tunnel. This means that these particular locations experience no lateral movement when subjected to static loads. However, at the right spring point and left spring point, the horizontal displacement ranges from 0.128 to 0.176 as a percentage of the tunnel diameter. This indicates that these points do undergo some lateral displacement due to static loading conditions.

Moving into the dynamic effects of earthquakes, three earthquake records are considered: Olympia earthquake, Northridge earthquake and Kalamata earthquake.

- The Olympia earthquake, characterized by a peak ground acceleration (PGA) of 0.16g and duration of 89.08 seconds, results in a significant maximum horizontal displacement ranging from 3.971 to 4.426, expressed as a percentage of the tunnel diameter. This indicates that the tunnel experiences substantial lateral movements during this earthquake event. The long duration contributes to the larger horizontal displacements observed.

- Similarly, the Northridge earthquake, which has a higher PGA of 0.883g but a shorter duration of 59.98 seconds, leads to a maximum horizontal displacement ranging from 0.645 to 1.242, expressed as a percentage of the tunnel diameter. Although the PGA is higher compared to the Olympia earthquake, the shorter duration results in comparatively smaller horizontal displacements. Nonetheless, it is important to note that these displacements are still significant and must be considered in the design and assessment of the tunnel's stability.

- Lastly, the Kalamata earthquake, with a PGA of 0.331g and duration of 25.88 seconds, produces a maximum horizontal displacement ranging from 0.188 to 0.391, as a percentage of the tunnel diameter. The lower PGA and shorter duration contribute to the relatively smaller displacements observed compared to the other earthquakes. However, these displacements are still non-negligible and can affect the overall behavior and structural integrity of the tunnel.

In summary, the analysis of the results illustrates that under dynamic earthquake effects, the tunnel experiences significant horizontal displacements at various points. The magnitude of these displacements depends on the characteristics of the earthquake, such as PGA and duration. It is crucial to consider these dynamic effects in the design, construction and evaluation of tunnels to ensure their stability and safety during seismic events.
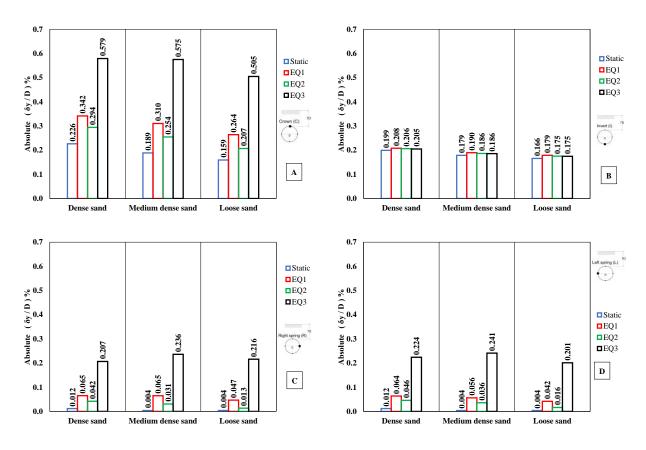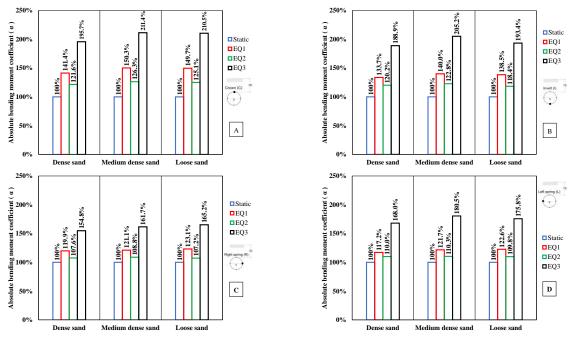
Fig. 14. Absolute maximum vertical displacements for different soil states subjected to static load and different earthquake records for (A) Crown point, (B) Invert point, (C) Right spring point and (D) Left spring point.

Fig. 14 show the absolute maximum vertical displacements for monitoring points as the percentage ratio of tunnel diameter (δ_y/D%) for different soil states under static load and earthquake records as follows:

- Crown Point: The vertical displacement at the crown point gradually decreases from dense to loose sand for both static loads and earthquake records. This suggests that denser soil states provide better resistance to vertical movement compared to looser soil states. The decrease in vertical displacement can be attributed to the increased soil stiffness and ability to withstand applied loads.

- Invert Point: The vertical displacement at the invert point is nearly equal for all types of soil and remains constant across both static and earthquake loading conditions. The displacement ranges from 0.166 to 0.208. This indicates that the invert point is relatively less affected by soil type and loading conditions, resulting in similar vertical displacements regardless of these factors.

- Right Spring Point and Left Spring Point: Under static loads, the vertical displacement at these points is relatively small, ranging from 0.004 to 0.012 as a percentage of the tunnel diameter. This indicates minimal vertical movement due to static loading conditions. However, under earthquake records, the maximum vertical displacement increases significantly. For the Northridge earthquake, with a PGA of 0.883g and duration of 59.98 seconds, the vertical displacement ranges from 0.201 to 0.241. For the Olympia earthquake, with a PGA of 0.16g and duration of 89.08 seconds, the vertical displacement ranges from

0.042 to 0.065. For the Kalamata earthquake, with a PGA of 0.331g and duration of 25.88 seconds, the vertical displacement ranges from 0.013 to 0.046. The dynamic effect of earthquakes significantly amplifies the vertical displacement at the spring points. This amplification can be attributed to the inertial forces generated during seismic waves, causing the soil and the tunnel structure to undergo larger vertical displacements compared to static loading conditions.

In summary analysis of the results shows that, although the crown point experiences reduced vertical displacement with denser soil, the invert point is not significantly affected. The spring points show minimal vertical displacement under static loads but undergo significant amplification during earthquakes.
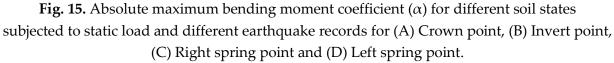

Fig. 15. Absolute maximum bending moment coefficient (α) for different soil states subjected to static load and different earthquake records for (A) Crown point, (B) Invert point, (C) Right spring point and (D) Left spring point.

Fig. 15 show the absolute maximum bending moment coefficient (α) of monitoring points for different soil states under static load and earthquake records as follows:

- Crown Point: The crown point experiences an increase in absolute bending moment under earthquake loading compared to static loads. For the Northridge earthquake, with a PGA of 0.883g and duration of 59.98 seconds, the increase ranges from 95.7% to 111.4%. Similarly, for the Olympia earthquake, with a PGA of 0.16g and duration of 89.08 seconds, the increase varies from 41.4% to 50.3%. For the Kalamata earthquake, with a PGA of 0.331g and duration of 25.88 seconds, the increase ranges from 21.6% to 26.3%.

  These findings indicate that earthquakes impose higher bending moments on the crown point of the tunnel compared to static loading conditions. The significant increases in the absolute bending moment coefficients suggest that seismic events induce additional forces and moments that lead to greater demands on the tunnel structure, particularly at the crown point.

- Invert Point: Similar to the crown point, the invert point experiences an increase in absolute bending moment under earthquake loading. Under the Northridge earthquake, the increase varies from 93.4% to 105.2% compared to static loads. For the Olympia earthquake, the increase ranges from 33.7% to 40%. For the Kalamata earthquake, the increase ranges from 18.4% to 22.8%.

  These results indicate that earthquakes generate higher bending moments at the invert point of the tunnel structure. The increase in absolute bending moment coefficients suggests that seismic events impose additional forces and moments on the tunnel, resulting in greater structural demands at the invert point.

- Right Spring Point and Left Spring Point: The right spring point and left spring point also experience an increase in absolute bending moment under earthquake loading. For the Northridge earthquake, the increase at the right spring point ranges from 54.8% to 65.2% compared to static loads. In the case of the Olympia earthquake, the increase ranges from 19.9% to 23.1%. For the Kalamata earthquake, the increase varies from 7.2% to 8.8%. Similarly, at the left spring point, the increase under the Northridge earthquake ranges from 68% to 80.5%, while for the Olympia earthquake, the increase ranges from 17.2% to 22.6%. For the Kalamata earthquake, the increase varies from 9.8% to 10.3%.

  These results indicate that earthquakes induce higher bending moments at both the right and left spring points of the tunnel structure. The increase in absolute bending moment coefficients suggests that seismic events impose additional forces and moments, leading to greater demands on the tunnel structure at these specific points.

In summary, analysis of the results shows that the behavior of the tunnel under the dynamic effect of earthquakes differs significantly from static loading conditions. The crown point, invert point and spring points of the tunnel experience increased bending moments during earthquakes.
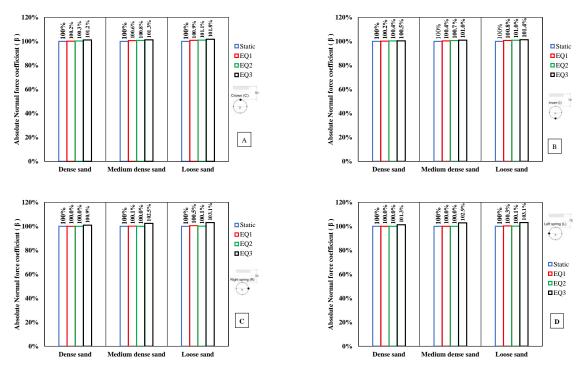

Fig. 16. Absolute maximum normal force coefficient (β) for different soil states subjected to static load and different earthquake records for (A) Crown point, (B) Invert point, (C) Right spring point and (D) Left spring point.

Fig. 16 show that the maximum normal force coefficient (β) of monitoring points for different soil states under static load and earthquake records is as follows:

-   Consistency across soil states: The maximum normal force coefficient (β) remains nearly constant for all types of soil (dense, medium dense and loose sand) under both static and earthquake loading conditions. This consistency suggests that the normal forces experienced by the tunnel structure at the monitoring points do not vary significantly with the soil state.
-   Earthquake Loading: Regardless of the soil type, the maximum normal force coefficient (β) remains relatively constant under earthquake loading conditions compared to static loads. This indicates that seismic waves do not significantly affect the normal forces experienced at the monitoring points of the tunnel structure.

Overall, the maximum normal force coefficient (β) of the tunnel monitoring points is not significantly influenced by soil type or the dynamic effect of earthquakes. This consistency indicates that the normal forces experienced by the tunnel structure remain relatively constant, regardless of the loading conditions or soil characteristics. It's important to note that while the normal forces may not vary significantly, other factors such as bending moments and displacements may still be affected by earthquakes and soil type.

5. Summary and Conclusions

In this study, circular tunnels were investigated under the influence of three different earthquake records (Olympia earthquake, Kalamata earthquake and Northridge earthquake) for different soil states. Three types of soil, ranging from dense sand to loose sand were studied. The earthquake records varying in PGA values (0.16 g to 0.883 g) and duration in addition to static loads have been considered. Specific points were observed to monitor deformations and stresses.

The most important results and conclusions are as follows:

1)   Dynamic horizontal displacement as a ratio of tunnel diameter ($\delta_x/D\%$), in the case of earthquake analysis, increases by 0.194 to 4.225 compared to static analysis for the crown point. While it increases by 0.188 to 4.193 for invert point and by 0.290 to 4.015 for the right spring point and by 0.352 to 4.426 for the left spring point.

2)   Dynamic vertical displacement as a ratio of tunnel diameter ($\delta_y/D\%$), in the case of earthquake analysis, increases by 0.207 to 0.579 compared to static analysis for the crown point. While it increases by 0.175 to 0.208 for invert point, and by 0.013 to 0.236 for the right spring point, and by 0.016 to 0.241 for the left spring point.

3)   Bending moment coefficient (α), in the case of earthquake analysis, increases by 21.60% to 111.40% compared to static analysis for the crown point. While it increases by 18.40% to 105.20% for invert point and by 7.20% to 65.20% for the right spring point and by 9.80% to 80.50% for the left spring point.

4)   Normal force coefficient (β), in the case of earthquake analysis, increases by 0.20% to 1.80% compared to static analysis for the crown point. While it increases by 0.20% to 1.40% for invert point and by 0.50% to 3.10% for the right spring point and by 0.30% to 3.10% for the left spring point.

5)   Axial forces remain nearly constant for earthquake records with PGA below 0.331g, but slightly increase for PGA exceeding 0.331g.

6) Duration for earthquake records has a greater impact on horizontal displacement than PGA values.

7) Peak ground acceleration has significant effects on vertical displacements, bending moments and axial forces.

Finally, the growing and increasing frequency and intensity of earthquakes led to the necessity of considering the effects of earthquake records on tunnel behaviour and design.

References

[1] Lee, I. M. and An, D. J. (2001). "Seismic analysis of tunnel structures". Journal of Korean Tunnelling and Underground Space Association, vol. 3, no. 4, pp. 3-15.

[2] Pakbaz, M. C. and Yareevand, A. (2005). "2-D analysis of circular tunnel against earthquake loading". Tunnelling and Underground Space Technology, vol. 20, no. 5, pp. 411-417.

[3] Arango, I. (2008). "Theme paper: earthquake engineering for tunnels and underground structures. a case history". In Geotechnical Earthquake Engineering and Soil Dynamics IV, pp. 1-34.

[4] Sun, Y., Klein, S., Caulfield, J., Romero, V. and Wong, J. (2008). "Seismic analyses of the Bay Tunnel. In Geotechnical Earthquake Engineering and Soil Dynamics IV pp. 1-11.

[5] Amorosi, A. and Boldini, D. (2009). "Numerical modelling of the transverse dynamic behaviour of circular tunnels in clayey soils". Soil Dynamics and Earthquake Engineering, vol. 29, no. 6, pp. 1059-1072.

[6] Asheghabadi, M. S. and Matinmanesh, H. (2011). "Finite element seismic analysis of cylindrical tunnel in sandy soils with consideration of soil-tunnel interaction". Procedia engineering, vol. 14, pp. 3162-3169.

[7] Abdel-Motaal, M. A., El-Nahhas, F. M. and Khiry, A. T. (2014). "Mutual seismic interaction between tunnels and the surrounding granular soil". HBRC Journal, vol. 10, no. 3, pp. 265-278.

[8] Hamdy, H. A., Enieb, M., Khalil, A. A. and Ahmed, A. S. (2015). "Seismic analysis of urban tunnel systems for the greater Cairo metro line No. 4". Electron. J. Geotech. Eng, vol. 20, pp. 4207-4222.

[9] Patil, M., Choudhury, D., Ranjith, P. G. and Zhao, J. (2018). "Behavior of shallow tunnel in soft soil under seismic conditions". Tunnelling and Underground Space Technology, vol. 82, pp. 30-38.

[10] De silva, F., Fabozzi, S., Nikitas, N., Bilotta, E. and Fuentes, R. (2021). "Seismic vulnerability of circular tunnels in sand". Géotechnique, vol. 71, no. 11, pp. 1056-1070.

[11] Zaid, M. and Mishra, S. (2021). "Numerical analysis of shallow tunnels under static loading: a finite element approach". Geotechnical and Geological Engineering, vol. 39, pp. 2581-2607.

[12] Alzabeebee, S. (2022). "A comparative study of the effect of the soil constitutive model on the seismic response of buried concrete pipes". Journal of Pipeline Science and Engineering, vol. 2, no. 1, pp. 87-96.

[13] Dong, S., Zhang, X., Jia, C., Li, S. and Wang, K. (2023). "Study on Seismic Response and Vibration Reduction of Shield Tunnel Lining in Coastal Areas". Sustainability, vol. 15, no. 5, pp. 4185.

[14] Shakya, R., Singh, M. and Samadhiya, N. K. (2023). "Response of Underground Tunnels to Combined Dynamic Loadings of Running Metro-train and Earthquake". Journal of Mining and Environment, vol. 14, no. 1, pp. 113-131.

[15] "PLAXIS 2D-Reference Manual V21". Brinkgreve, R. and Vermeer, P. A. (2021). https://communities.bentley.com/products/geotech-analysis/w/wiki/46137/manuals---plaxis (accessed on 5 January 2022).

[16] Earthquake records https://www.eng.ucy.ac.cy/petros/Earthquakes/earthquakes.htm (accessed on 5 January 2023).

[17] Hefny, A. M., Chua, H. C. and Zhao, J. (2004, July). "Parametric studies on the interaction between existing and new bored tunnels". In Tunnelling and Underground Space Technology. Underground Space For Sustainable Urban Development. Proceedings of The 30th Ita-Aites World Tunnel Congress Singapore, 22-27 MAY 2004, vol. 19, no. 4-5.

[18] Kim, S. H. and Kim, S. H. (1996). "Model testing and analysis of interactions between tunnels in clay" (Doctoral dissertation, University of Oxford).